

Computer simulation of cw Doppler wind lidar operation in the turbulent atmosphere

V.A. Banakh, Ch. Werner, N.P. Krivolutskii, and I.N. Smalikhov

*Institute of Atmospheric Optics,
Siberian Branch of the Russian Academy of Sciences, Tomsk*

Received August 5, 1999

The algorithms simulating cw Doppler wind lidar operation in the turbulent atmosphere are described in the paper. The algorithms are realized in the LabView environment. The computer codes include parts simulating the atmospheric turbulence, lidar return signal, and signal processing to extract information on the mean wind and its turbulent characteristics. The codes developed are a virtual tool allowing one to perform effective statistical planning of experiments on sounding the wind turbulent field under different conditions in the atmospheric boundary layer.

1. Introduction

The cw Doppler lidars developed at present are intended, first of all, for studying the dynamic processes in the boundary layer of the atmosphere.¹⁻⁶ Such systems when equipped with a beam steering device to scan the atmospheric volume under study allow one to measure three components of the wind velocity vector at different heights and then to reconstruct the height profiles of the mean velocity. Results of theoretical and experimental investigations⁵⁻⁷ formed a basis for the development of an optimal procedure of reconstruction of height profiles of the mean wind velocity allowing for a state of the atmospheric boundary layer.

Along with measurements of the mean wind velocity a cw Doppler lidar can also be used to measure parameters of the dynamic turbulence such as the rate of turbulent energy dissipation, wind velocity variance, outer scale of turbulence, and vertical turbulent momentum flux. A description of the methods developed for measurements of these turbulent parameters with a scanning cw Doppler lidar can be found in Refs. 8-11. In this papers one can also find examples of reconstruction of the height profiles of turbulence parameters from the experimental data. However, the problems in providing desired accuracy of the Doppler lidar measurements of turbulence parameters and choosing optimal procedures of sounding (geometry and measurement time) depending on the thermodynamic state of the atmospheric boundary layer are still to be studied in a more detail. It is obvious that comparative experiments using sensors at a meteorology mast are only possible in the lower part of the boundary layer up to the altitude determined by the mast height.

In this paper we propose a method that is based on numerical simulations of a Doppler lidar operation for studying the accuracy of measuring the atmospheric turbulence parameters in the boundary layer of the atmosphere. In so doing we set the profiles of the parameters sought and then simulate random samples of lidar measurement data. Thus simulated data are then

processed and the variance of deviations of estimated values from the initially set reference profiles of the parameters sought is calculated.

2. Simulation algorithm

Figure 1 shows the geometry of conical scanning with a laser beam used in measurements with a cw Doppler lidar. In this optical arrangement the beam moves along a conical surface about the vertical axis z at an angle φ with respect to the horizontal plane $\{x, y\}$ at an angular velocity ω_0 . Here θ denotes the azimuth angle as a function of time t , i.e., $\theta = \omega_0 t$. By focusing the beam at a distance R a volume sounded is formed, with its center at the height $h \approx R \sin \varphi$.

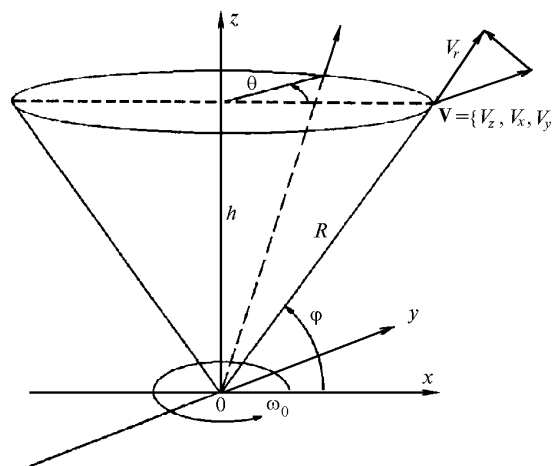


Fig. 1. Geometry of a sounding with a scanning lidar.

From a single measurement in time $t = \theta / \omega_0$ one can estimate only a radial component of the wind velocity vector $V_r(z', \theta)$ which is related to the components of velocity vector $\mathbf{V}(\mathbf{r}, t) = \{V_x, V_y, V_z\}$ at a fixed point $\mathbf{r} = \{x, y, z\}$ in time t by the relation

$$V_r(z', \theta) = \mathbf{sV}(z', \theta / \omega_0), \quad (1)$$

where $z' = |\mathbf{r}|$ is the distance from the lidar to the observation point; $\mathbf{s} = \{\sin \varphi \cos \theta, \sin \varphi \sin \theta, \cos \varphi\}$.

In successively scanning during equal time intervals t_0 one obtains Doppler spectra of the recorded signal power $W(f, mt_0)$, where f is the frequency; $m = 1, 2, 3, \dots$ is the number of the spectrum obtained. An estimate of such a spectrum is obtained by averaging individual (not smoothed) spectra measured during the time $t_s = 1/\Delta f$, where Δf is the frequency resolution. To decrease a level of fluctuations in the spectrum estimated that are caused by both the random variations of scattered wave field and system noise, one normally uses from one hundred to one thousand spectra in such an averaging. For example, at $\Delta f = 20$ kHz and the number of individual spectra averaged $N_a = 1000$ the time of measuring one spectrum is $t_0 = N_a/\Delta f = 50$ ms.

With the account for the Doppler formula $\Delta f = (2/\lambda)\Delta V$, where ΔV is the speed; λ is the wavelength; the Doppler spectrum is represented in the form

$$W(k\Delta V, m\Delta\theta) = W_s(k\Delta V, m\Delta\theta) + W_n(k\Delta V, m\Delta\theta), \quad (2)$$

where $k = 1, 2, \dots$ is the number of the spectral channel; $\Delta\theta = \omega_0 t_0$ is the resolution in the azimuth angle. The first term in Eq. (2) is the power spectrum of the recorded signal, which is completely averaged over its fluctuations with the distribution of the scattering particles' velocities in the volume sounded being unchanged ("frozen turbulence"). The second term describes the fluctuations of the spectrum estimated, their level being determined by the signal-to-noise ratio and by the time t_0 of the spectrum measurements.

When the volume sounded contains sufficiently large number of particles that scatter quite effectively, the effect of the second term in Eq. (2) on the value of the estimated velocity can be neglected. Having this in mind and that such a situation occurs quite often in the boundary layer, the simulated results corresponding to the case when the estimated power spectrum of a signal coincides with $W_s(k\Delta V, m\Delta\theta)$ are presented below. Based on the results from Ref. 12 the spectrum $W_s(k\Delta V, m\Delta\theta)$ can be written in the form

$$W_s(k\Delta V, m\Delta\theta) = \frac{\Delta r}{\Delta V} \sum_{i=0}^{M'-1} Q_s(\Delta r i) \operatorname{sinc}^2 \left\{ \pi \left(k - \frac{|V_r(\Delta r i, m\Delta\theta)|}{\Delta V} \right) \right\}, \quad (3)$$

where Δr is the spatial resolution along the optical axis z' ; $Q_s(\Delta r i) = \{(\pi k_0 a_0^2) ((1 - z'/R)^2 + (\Delta r i)^2 / (k_0 a_0^2))\}^{-1}$ is the weighting function characterizing a contribution of each segment M' of the path with the length Δr to the normalized signal power ($\Delta r \sum_{i=0}^{M'-1} Q_s(\Delta r i) = 1$); a_0 is the initial radius of laser beam in the plane $z' = 0$; $k_0 = 2\pi/\lambda$, $\operatorname{sinc}(x) = \sin(x)/x$, $k = 1, 2, \dots, M_D - 1$ (M_D is the number of the spectral channels); $m = 1, 2, \dots, M_s$ (M_s is the total number of measured spectra). When the frequency of the reference and sounding beams coincide (homodyne lidar system), as is the case considered here, it is necessary that the radial component of the velocity $V_r(\Delta r i, m\Delta\theta)$ in Eq. (3) be taken by modulus.

To estimate the velocity $V_D(m\Delta\theta)$ from the Doppler spectrum $W_s(k\Delta V, m\Delta\theta)$, we use the following relationship:

$$V_D(m\Delta\theta) = \Delta V \left[k_{\max} + \sum_{k=k_1}^{k_1} k W_s((k_{\max} + k) \Delta V, m\Delta\theta) / \hat{S} \right], \quad (4)$$

where k_{\max} is the number of the spectral channel corresponding to the spectrum maximum; $[\Delta V(k_{\max} - k_1), \Delta V(k_{\max} + k_1)]$ is the interval of velocities, within which the value V_D is being estimated;

$\hat{S} = \sum_{k=k_1}^{k_1} W_s((k_{\max} + k) \Delta V, m\Delta\theta)$. It is obvious that the index k_1 introduced here must satisfy the following conditions:

$$k_1 \leq k_{\max}, \quad (5)$$

$$k_{\max} + k_1 \leq M_D - 1. \quad (6)$$

To select k_1 , we introduce a concept of the effective spectrum width σ_s (in the units of speed) determined, for example, from the fall off of the spectrum $W_s(k\Delta V)$ down to the level $W_s(k\Delta V)/2$ when moving off from the spectrum maximum or as the second central moment of the velocity.¹¹ Then we require the following conditions to hold:

$$\sigma_s \ll k_{\max} \Delta V, \quad (7)$$

$$\sigma_s \ll (M_D - 1 - k_{\max}) \Delta V; \quad (8)$$

$$\Delta V \ll \sigma_s; \quad (9)$$

and

$$\sigma_s \ll k_1 \Delta V. \quad (10)$$

The conditions (5)–(10) allow one, after substituting expression (3) into Eq. (4), passing from summation over k to the integration over V ($\Delta V k \rightarrow V$) and changing of $\operatorname{sinc}^2(\pi(V - |V_r|)/\Delta V)$ for $\Delta V \delta(V - |V_r|)$, where $\delta(x)$ is the delta function, to obtain the following expression:

$$V_D(m\Delta\theta) = \Delta r \sum_{i=0}^{M'-1} Q_s(\Delta r i) |V_r(\Delta r i, m\Delta\theta)|. \quad (11)$$

To correctly estimate the velocity V_D from the data of field measurements, certain *a priori* information on the wind direction is needed. In simulating numerically this task we select the wind direction and therefore we can omit the sign of modulus of the value V_r in Eq. (11). Let us suppose that the selected step Δr of sampling along the optical axis z' satisfies the conditions that $\Delta r \ll \Delta z$, where $\Delta z = (\lambda/2)(R/a_0)^2$ is the effective longitudinal dimension of the volume sounded,¹¹ and $M'\Delta r > 2R$. Then the summation in the expression (11) can be changed for integration. As a result, we have:

$$V_D(m\Delta\theta) = \int_0^{\infty} dz' Q_s(z') V_r(z', m\Delta\theta). \quad (12)$$

Thus, when the conditions (5) to (10) hold, the velocity estimated from the data of numerical simulation will be

the radial component of wind velocity which is averaged over volume sounded.

During the conical scanning a change of wind direction relative to the projection of a sounding beam on the horizontal plane occurs and the radial wind velocity component changes, correspondingly, its sign at a certain moment in time. It is obvious that at certain azimuth angles $m\Delta\theta$, when V_r is close to zero, the conditions (7) and (10) cannot be satisfied. For such angles one can either make a more rough estimation of the radial wind velocity by assigning $k_1 \leq k_{\max}$ in Eq. (4) (however, in this case, as a rule, a problem on determination of the sign of V_D arises) or remove that uncertain estimates from the data array intended for further processing to determine the parameters sought.

In accordance with Eq. (3) one has, in order to obtain the Doppler spectra at different azimuth angles $\theta = m\Delta\theta$, to simulate random samples of the radial wind velocity $V_r(z', \theta)$ connected with the three components of the wind velocity vector $\mathbf{V}(\mathbf{r}, t)$ through formula (1). Simulation of three-dimension random field of the three velocity components with a desired spatial resolution is impossible to be performed on modern personal computers due to the limited internal memory and performance. Therefore a simplified algorithm was used to simulate the radial wind velocity.

Let us represent $V_r(\Delta r_i, m\Delta\theta)$, allowing for Eqs. (11) and (12), in the form

$$V_r(\Delta r_i, m\Delta\theta) = V_D(m\Delta\theta) + \Delta V_r(\Delta r_i), \quad (13)$$

where

$$\begin{aligned} \Delta V_r(\Delta r_i) = & \tilde{V}_r(R_m + \Delta r_i) - \\ & - \Delta r \sum_{i=0}^{M'-1} Q_s(\Delta r_i) \tilde{V}_r(R_m + \Delta r_i); \end{aligned} \quad (14)$$

$\tilde{V}_r = V_r - \langle V_r \rangle$ are the fluctuations of the radial wind velocity; $R_m = \Delta r N_m$; $N_m = [2R \cos\varphi (m - 1)\Delta\theta / \Delta r]$. Fluctuations of the velocity V_D are determined, on the whole, by the turbulent vortices with the size $l > \Delta z$, and ΔV_r is determined by the small-scale turbulence ($l < \Delta z$). This allows one to consider the random processes V_D and \tilde{V}_r as independent ones and simulate them separately.

The velocity $V_D(m\Delta\theta)$ was simulated in the region of the azimuth angles θ using the following expression for the correlation function: $B_D(\theta_m, \theta_l) = \langle \tilde{V}_D(\theta_m) \times \tilde{V}_D(\theta_l) \rangle$, where $\tilde{V}_D = V_D - \langle V_D \rangle$, which was found under the assumption on the stationarity, horizontal homogeneity, and isotropy of wind velocity field and "frozen" turbulent inhomogeneities¹³:

$$\begin{aligned} B_D(\theta_m, \theta_l) = & \int_0^\infty \int_0^\infty dz' dz'' Q_s(z') Q_s(z'') \times \\ & \times \sum_{i=1}^3 \sum_{k=1}^3 S_i(\Delta\theta_m) S_k(\Delta\theta_l) B_{ik}(z' \mathbf{S}(\theta_m) - z'' \mathbf{S}(\theta_l) + \end{aligned}$$

$$+ \langle \mathbf{V} \rangle (\theta_m - \theta_l) / \omega_0), \quad (15)$$

where $S_1 = \sin\varphi$, $S_2 = \cos\varphi \cos\theta$, $S_3 = \cos\varphi \sin\theta$; $B_{ik}(\mathbf{r}) = \langle \tilde{V}_i(\mathbf{r}_1 + \mathbf{r}) \tilde{V}_k(\mathbf{r}_1) \rangle$ is the spatial correlation tensor of wind velocity fluctuations; $\tilde{V}_1 \equiv \tilde{V}_z$, $\tilde{V}_2 \equiv \tilde{V}_x$, and $\tilde{V}_3 \equiv \tilde{V}_y$. In the isotropic case of a solenoid-like field of velocities for $B_{ik}(\mathbf{r})$ we have¹³:

$$B_{ik}(\mathbf{r}) = B_V(r) \delta_{ik} + \frac{r}{2} \frac{dB_V(r)}{dr} \left(\delta_{ik} - \frac{r_i r_k}{r^2} \right), \quad (16)$$

where $B_V(r)$ is the longitudinal correlation function of wind velocity; $r = |\mathbf{r}|$; δ_{ik} is the Kronecker symbol. As the model of $B_V(r)$, simple expression was used

$$B_V(r) = \sigma_V^2 \exp[-1.21(r/L_V)^{2/3}], \quad (17)$$

where $\sigma_V^2 = B_V(0)$ is the variance; $L_V = \int_0^\infty dr B_V(r) / \sigma_V^2$

is the integral scale of correlation of the wind velocity fluctuations (the outer scale of turbulence). Since in the inertial interval of turbulence ($r \ll L_V$) the structure function of the velocity $D_V(r) = 2[\sigma_V^2 - B_V(r)]$ is determined by the expression¹³:

$$D_V(r) = C_k \varepsilon^{2/3} r^{2/3}, \quad (18)$$

where $C_k \approx 2$ is the Kolmogorov constant; ε is the velocity of turbulent energy dissipation, then one can easily find from Eqs. (17) and (18) the expression that relates σ_V , L_V , and ε :

$$\varepsilon = \left(\frac{2 \cdot 1.21}{C_k} \right)^{3/2} \frac{\sigma_V^2}{L_V}. \quad (19)$$

Random samples of $V_D(m\Delta\theta)$ were simulated by the method of linear transformation¹⁴:

$$V_D(m\Delta\theta) = \langle V_D(m\Delta\theta) \rangle + \sum_{m'=1}^m a_{mm'} \xi_{m'}, \quad (20)$$

where elements of the matrix $a_{mm'}$ are connected with the elements of the correlation matrix $B_D(m\Delta\theta, l\Delta\theta)$ by the following relationship:

$$B_D(m\Delta\theta, l\Delta\theta) = \sum_{m'=1}^m a_{mm'} a_{lm'}. \quad (21)$$

In Eq. (20) ξ_m is the pseudo-random value distributed according to the normal law with the zero mean value and unit variance, and $\langle \xi_m \xi_{m'} \rangle = \delta_{mm'}$.

To simulate random samples of the radial velocity $\tilde{V}_r(i\Delta r)$, we have also used the model (17), but in contrast to $V_D(m\Delta\theta)$, for which the $B_D(\theta_m, \theta_l)$ is not the function of difference of two arguments, here we have a possibility of using a more efficient algorithm. After numerical calculations of the spectrum

$$S_V(\alpha) = \int_0^\infty dr B_V(r) e^{-2\pi j \alpha r} \quad (22)$$

samples of $\tilde{V}_r(i\Delta r)$ were simulated in the spectral region using fast Fourier transform:

$$\tilde{V}_r(i\Delta r) = \text{Re} \left\{ \sum_{k=0}^{N-1} \xi_k \left[\frac{1}{2N\Delta r} S_V \left(\frac{k}{N\Delta r} \right)^{1/2} \exp \left(2\pi j \frac{k i}{N} \right) \right] \right\}, \tag{23}$$

where ξ_k is the pseudo-random value that is distributed according to the normal law and satisfies the following conditions: $\langle \xi_k \xi_{k'} \rangle = 0$, $\langle \xi_k \xi_{k'}^* \rangle = \delta_{kk'}$. In expression (23) $S_V(k)$ must be symmetric relative to the Nyquist frequency: $S_V(k) = S_V(N - k)$.

3. Simulated results

In simulating Doppler spectra, the following parameters of a lidar were accepted: the wavelength $\lambda = 10.6 \mu\text{m}$, the initial radius of sounding beam $a_0 = 7.5 \text{ cm}$. Figure 2 presents examples of simulation of the Doppler spectra $W_s(V)$ for $\langle V_r \rangle = 10 \text{ m/s}$ and various R , σ_V , and L_V . It is obvious that an increase in R or σ_V , and also a decrease in L_V lead to the spectrum broadening. Dashed lines in the figure show the estimates of the velocity using Eq. (4). The more asymmetric the spectral distribution is the stronger such an estimate differs from $\Delta V k_{\text{max}}$.

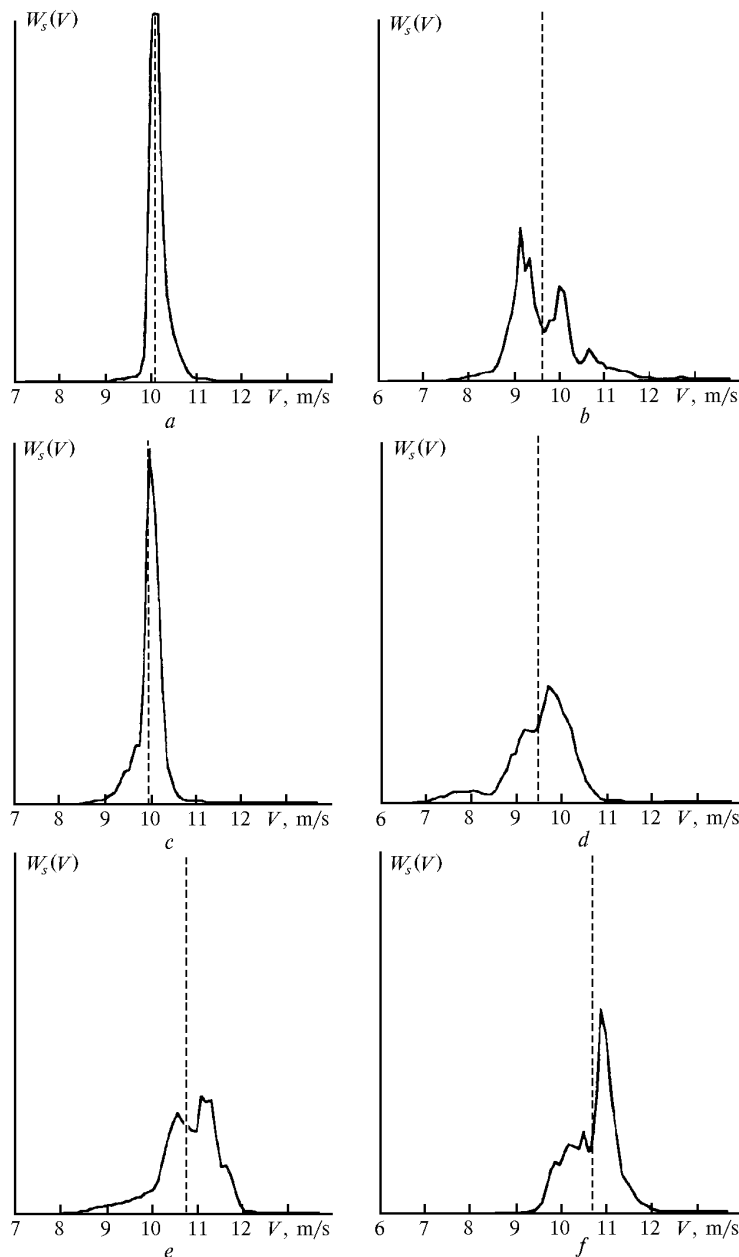


Fig. 2. Examples of simulation of the Doppler spectra $W_s(V)$ for $\langle V_r \rangle = 10 \text{ m/s}$ and $\sigma_V = 0.5 \text{ m/s}$, $L_V = 100 \text{ m}$, $R = 100 \text{ m}$ (a); $\sigma_V = 1.5 \text{ m/s}$, $L_V = 100 \text{ m}$, $R = 100 \text{ m}$ (b); $R = 50 \text{ m}$, $\sigma_V = 1 \text{ m/s}$, $L_V = 100 \text{ m}$ (c); $R = 500 \text{ m}$, $\sigma_V = 1 \text{ m/s}$, $L_V = 100 \text{ m}$ (d); $L_V = 30 \text{ m}$, $\sigma_V = 1 \text{ m/s}$, $R = 200 \text{ m}$ (e); $L_V = 300 \text{ m}$, $\sigma_V = 1 \text{ m/s}$, $R = 200 \text{ m}$ (f).

Once the estimates of the velocity have been obtained at different azimuth angles during one scanning cycle those have been fitted by least squares method, in accordance with Eq. (1), to the dependence $\hat{V}_r(m\Delta\theta) = \sin\varphi \hat{V}_z + \cos\varphi [\cos(m\Delta\theta)\hat{V}_x + \sin(m\Delta\theta)\hat{V}_y]$, wherefrom the estimates of the three components of the wind velocity vector $\hat{V} = \{\hat{V}_z, \hat{V}_x, \hat{V}_y\}$ were determined.

Simulation of the scanning lidar operation was performed under condition that one complete turn of a sounding beam about the vertical axis occurs during the time $T = 7$ s, and the time of measurement of one Doppler spectrum is $t_0 = 50$ ms. Then a number of simulated spectra is $N_{sp} = T/t_0 = 140$, and resolution in the azimuth angle is $\Delta\theta = \omega_0 t_0 = 2\pi t_0/T \approx 2.57^\circ$. The spectra $W_s(V)$ whose maxima are in the range $\Delta V k_{max} < 1$ m/s were neglected and therefore the number of the obtained estimations of the velocity $N_V < N_{sp}$. It is obvious that the smaller the mean wind velocity or the larger the angle φ , the smaller is the N_V number.

Figure 3 presents an example of the dependence $V_D(m\Delta\theta)$ obtained from the simulated data on Doppler spectrum. The dependence $\hat{V}_r(m\Delta\theta)$ is shown by dashed line, and $\langle \hat{V}_r(m\Delta\theta) \rangle$ by the solid line. Here the values of the vector components $\langle \mathbf{V} \rangle$ and \hat{V} are given.

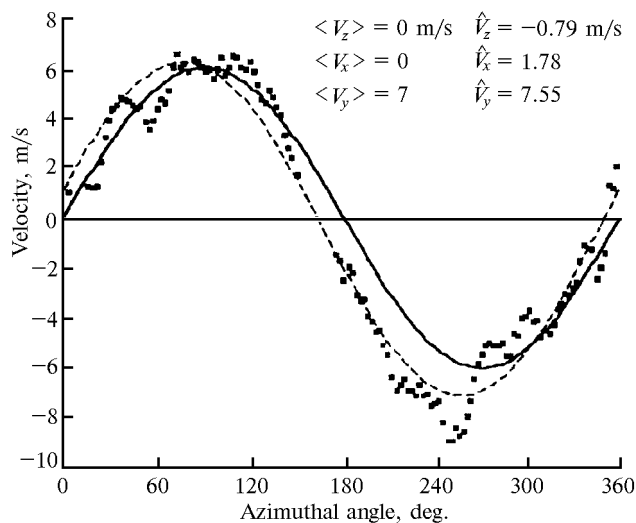


Fig. 3. An example of estimating Doppler spectra of $V_D(m\Delta\theta)$ (dots), $\hat{V}_r(m\Delta\theta)$ (dashed curve) from simulated data; solid curve is $\langle \hat{V}_r(m\Delta\theta) \rangle$.

From the data of numerical simulations assuming different number of scans at a height h the rate of turbulent energy dissipation ϵ , wind velocity variance σ_V^2 , and the outer scale of turbulence L_V were determined. Description of the methods used to determine these parameters from measurement data obtained with a cw Doppler lidar can be found in Refs. 8–11. Here we would only note that ϵ is estimated by analyzing the deviations $V_D(m\Delta\theta) - \hat{V}_r(m\Delta\theta)$, and to obtain information on σ_V^2 it is also necessary to know the mean width of the Doppler spectra and the variance

of deviations of a single estimate of the wind velocity (for one scan) from the spectrum averaged over all scans.

From the estimations of ϵ and σ_V obtained by formula (19) the outer scale of turbulence $L_V = c\sigma_V^2/\epsilon$ is calculated, where the numerical coefficient $c = (2.121/C_k)^{3/2} \approx 1.33$ for the model of longitudinal correlation function of wind velocity used here. For example, if we use the model by von Karman¹³ $c \approx 0.67$. Thus, besides the statistical factors the accuracy of determination of the outer scale of turbulence L_V from the Doppler lidar data will also be determined by the degree to which the selected model of correlation function of the wind velocity corresponds to real situation.

The measurements in the atmosphere with a cw Doppler lidar aimed at reconstruction of the height profiles of turbulence^{9,10} have been conducted, as a rule, in succession at every of the selected heights (the height was given by change R or φ , $h = R \sin\varphi$). Normally one or several continuous complete scans (no more than three) were performed at each height. Then in the pre-determined time intervals $T_m \sim 2\text{--}5$ min the procedure was repeated many times. During T_m the turbulence could change essentially and thus obtained estimates of turbulent parameters can be considered as statistically independent. By analogy with the field experiments at fixed heights h_i where $i = 1, 2, \dots, 6$, we simulated the independent arrays of Doppler spectra. In this case the angle $\varphi = 30^\circ$ was kept the same for all heights. Every array corresponded to the set of spectra measured during one complete scan.

The reconstructed profiles were the profiles of the mean wind velocity $U(h)$, the rate of turbulent energy dissipation $\epsilon(h)$, wind velocity variance $\sigma_V^2(h)$, and the outer scale of turbulence $L_V(h)$ calculated in accordance with the models⁶ (Table 1).

Table 1

Number of the curve (Figs. 6 and 7)	h , m	U , m/s	σ_V , m/s	L_V , m	ϵ , m^2/s^3
1	50	6.90	1.23	133	0.018
2	100	7.77	1.20	200	0.011
3	200	8.63	1.15	266	0.0077
4	300	9.14	1.11	300	0.0060
5	400	9.50	1.07	320	0.0050
6	500	9.78	1.02	333	0.0043

Figure 4 shows the examples of reconstruction of the profiles of the rate of turbulent energy dissipation from the data of numerical simulations for five scans at the each of the levels h_i . The bold curve is the profile of $\epsilon(h_i)$ presented in Table 1. It is obvious that estimations of the turbulent energy dissipation rate $\hat{\epsilon}(h_i)$ are concentrated about the initial profile $\epsilon(h_i)$, i.e., no regular displacement of the estimations $\hat{\epsilon}(h_i)$ occurs.

To calculate the relative error of the estimation of the rate of turbulent energy dissipation $\sigma_\epsilon = [\langle (\hat{\epsilon} - \epsilon)^2 \rangle]^{1/2} / \epsilon$ 1000 independent estimations of $\hat{\epsilon}$

obtained from the data of the numerical simulation were used. Figure 5 presents the dependences of relative error σ_ϵ on the number N of scans for the heights h_i given in Table 1. It is obvious that the values of σ_ϵ at different heights are slightly different and with the increase of N (the bulk of the data processed) they decrease down to the level $\sim 18\%$ at $N = 10$.

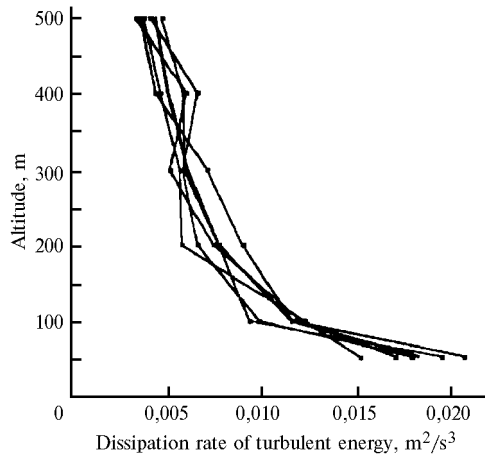


Fig. 4. Examples of the reconstruction of the height profiles of the rate of turbulent energy dissipation from the simulated data for 5 scans. Bold curve is the initial (reconstructed) profile of the dissipation rate $\epsilon(h)$.

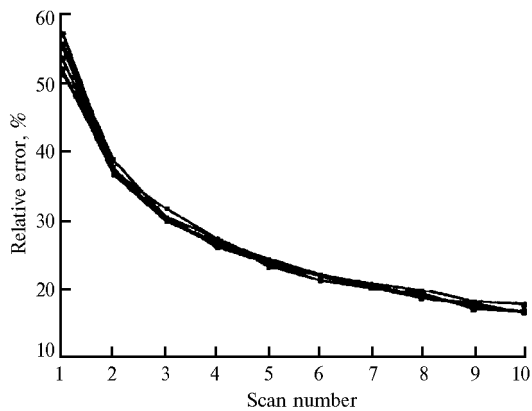


Fig. 5. The relative error of estimation of the rate of turbulent energy dissipation as a function of the number of scan samples.

Figure 6 shows the calculated results on the relative error of estimation of the wind velocity variance $\sigma_{\sigma_V^2} = [\langle (\hat{\sigma}_V^2 - \sigma_V^2)^2 \rangle]^{1/2} / \sigma_V^2$. Numbers at curves correspond to sounding height h_i given in Table 1. In contrast to σ_ϵ , the errors $\sigma_{\sigma_V^2}$ are different at the different heights. The lower the height h_i is, the higher the relative error of estimation of the wind velocity variance is. Such a behavior of $\sigma_{\sigma_V^2}$ can be understood if it is taken into account that one of the terms in the formula for estimating the variance $\hat{\sigma}_V^2$ is the mean square of the

Doppler spectrum width.^{9,10} The higher the height h_i is at a fixed angle φ , the larger is the longitudinal dimension of the volume sounded Δz and, therefore, the larger the turbulent vortices will contribute to the Doppler spectrum broadening thus making it more informative with regard to random variations of the wind velocity in the volume sounded (compare Figs. 2c and 2d). As it follows from Fig. 6, at the number of scans $N = 10$ the value of $\sigma_{\sigma_V^2}$ is within 17–25%.

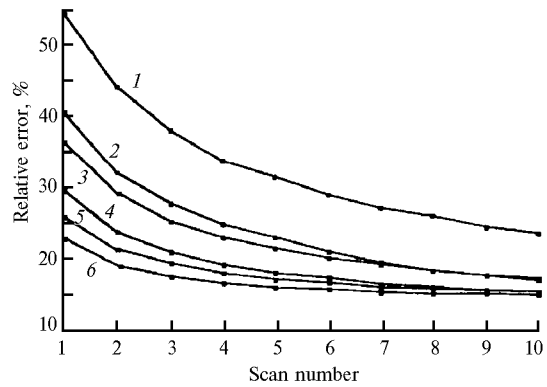


Fig. 6. The relative error of estimation of wind velocity variance as a function of the number of scans. Numbers at the curves correspond to the heights presented in Table 1.

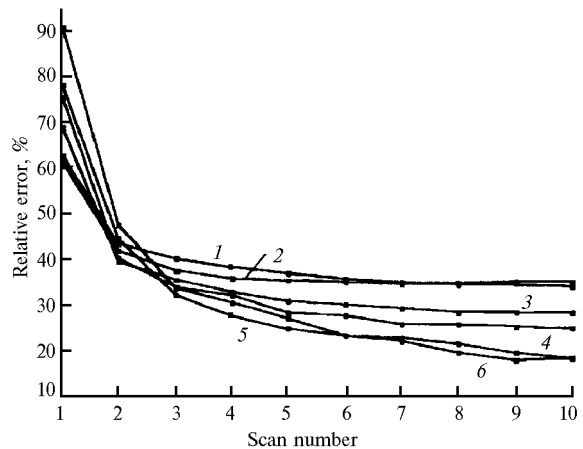


Fig. 7. The relative error of estimation of the outer scale of turbulence as a function of the number of scans. Numbers at the curves correspond to the heights presented in Table 1.

The values $\hat{\sigma}_V$ and $\hat{\epsilon}$ allow one to estimate the outer scale of turbulence by the formula $\hat{L}_V = 1.33\hat{\sigma}_V^3/\hat{\epsilon}$. Figure 7 shows the relative error of estimation of the outer scale of turbulence $\sigma_{L_V} = [\langle (\hat{L}_V - L_V)^2 \rangle]^{1/2} / L_V$ at different heights h_i . The numbers at the curves correspond to the notations in Fig. 6. It is obvious that the error in estimation \hat{L}_V is caused by random variations $\hat{\sigma}_V$ and $\hat{\epsilon}$, therefore the error σ_L exceeds the corresponding values of σ_ϵ and $\sigma_{\sigma_V^2}$ (compare Figs. 7, 5, and 6). At $N = 10$ the value of σ_L is within ~ 20 –40%.

4. Conclusion

In this paper we have discussed the algorithm of simulating the spectra measured with a cw Doppler lidar when scanning with the sounding beam along a cone. Based on the methods of lidar measurements of the atmospheric turbulence parameters that were developed in Refs. 8–11, the algorithms for estimating the rate of turbulent energy dissipation, variance of the wind velocity fluctuations, and the outer scale of turbulence from the simulated data have been constructed.

Analysis of the accuracy of reconstructing the height profiles of turbulent parameters that were preset according to Ref. 6 has been performed. The errors in determination of the turbulent parameters which are calculated from the simulated data conforms to the estimates of such errors in a field experiment. In particular, as was shown in Ref. 15, at 10 scans the measurement error in the rate of turbulent energy dissipation, in the case of nearly neutral temperature stratification of the atmosphere, is about 20%.

The developed algorithm for calculation of the Doppler spectra and the computer codes written in the LabView language do, as a matter of fact, comprise a virtual tool for simulating the operation of a cw Doppler scanning lidar. This allows one to perform a statistical planning of experiments on sounding the wind turbulent field under different conditions in the atmospheric boundary layer.

Acknowledgments

This study was carried out under partial financial support from the Russian Foundation for Basic Research (Grant 98–05–03131).

References

1. T.R. Lawrence, D.J. Wilson, C.E. Craver, I.P. Jones, R.M. Huffaker, and J.A. Thomson, *Rev. Sci. Instrum.* **43**, 512–518 (1972).
2. F. Köpp, R.L. Schwiesow, and Ch. Werner, *J. Climate Appl. Meteorol.* **3**, No. 1, 148–151 (1984).
3. V.M. Gordienko, A.A. Kormakov, L.A. Kosovsky, N.N. Kurichkin, G.A. Pogosov, A.V. Priezhev, and Y.Y. Putivskii, *Optical Engineering* **33**, No. 10, 3206–3213 (1994).
4. G.M. Ancellet, R.I. Menzies, and W.B. Grant, *J. Atmos. Oceanic Technol.* **6**, No. 1, 50–58 (1989).
5. F. Köpp, Ch. Werner, R. Haring, V.A. Banakh, I.N. Smalikho, and H. Kambezidis, *Contributions to Atmospheric Physics* **67**, No. 4, 269–286 (1994).
6. V.A. Banakh, I.N. Smalikho, F. Köpp, and Ch. Werner, *Appl. Optics* **34**, No. 12, 2055–2067 (1995).
7. V.A. Banakh, Ch. Werner, F. Köpp, and I.N. Smalikho, *Atmos. Oceanic Opt.* **6**, No. 11, 786–793 (1993).
8. V.A. Banakh, Ch. Werner, F. Köpp, and I.N. Smalikho, *Atmos. Oceanic Opt.* **9**, No. 10, 849–854 (1996).
9. V.A. Banakh, Ch. Werner, F. Köpp, N.P. Krivolutskii, and I.N. Smalikho, in: *Abstracts of Reports at the IVth Symposium on Atmospheric and Oceanic Optics*, Tomsk (1997) pp. 163–164.
10. V.A. Banakh, N.P. Krivolutskii, I.N. Smalikho, F. Köpp, and Ch. Werner, in: *Abstracts of Reports at the 19th International Laser Radar Conference*, Hampton (1998) pp. 727–729.
11. V.A. Banakh and I.N. Smalikho, *Atmos. Oceanic Opt.* **10**, Nos. 4–5, 295–302 (1997).
12. I.N. Smalikho, *Atmos. Oceanic Opt.* **8**, No. 10, 788–793 (1995).
13. I.L. Lumley and H.A. Panofsky, *The Structure of Atmospheric Turbulence* (Interscience, N. Y., 1964), 264 pp.
14. V.V. Bykov, *Numerical Simulation in Statistical Radiophysics* (Sov. Radio, Moscow, 1971), 326 pp.
15. V.A. Banakh, I.N. Smalikho, F. Köpp, and Ch. Werner, *J. Atmos. Oceanic Technol.* (1999), to be published.